Research Square

Preprints are preliminary reports that have not undergone peer review.
They should not be considered conclusive, used to inform clinical practice,
or referenced by the media as validated information.

Fungal–Fungal Interactions Drive Metabolic Reprogramming in Root-Associated Endophytes of *Salvia abrotanoides*

Yeganeh Teimoori-Boghsani
Ferdowsi University of Mashhad
Ali Ganjeali
ganjeali@um.ac.ir
Ferdowsi University of Mashhad
Gabriele Berg
Graz University of Technology
Tomislav Cernava
Graz University of Technology
Javad Asili
Mashhad University of Medical Sciences
Fatemeh Masoudi-Khorasani
Islamic Azad University, Mashhad
Nasrin Moshtaghi
Ferdowsi University of Mashhad

Research Article

Keywords: Endophytic fungi, Salvia abrotanoides, Cryptotanshinone, Co-culture, Secondary metabolites, Fungal communication

Posted Date: July 9th, 2026

DOI: https://doi.org/10.21203/rs.3.rs-10063911/v1

License: This work is licensed under a Creative Commons Attribution 4.0 International License.
Read Full License

Additional Declarations: No competing interests reported.

Abstract

Root-associated endophytic fungi are integral components of plant holobionts, where interspecific interactions shape ecological fitness and secondary metabolism. In this study, five fungal endophytes isolated from the roots of *Salvia abrotanoides*—*Paraphoma radicina*, *Penicillium murcianum*, *Penicillago nodositata*, *Penicillium canescens*, and *Coniolariella hispanica*—were investigated to evaluate how fungal–fungal interactions influence metabolic expression under co-culture conditions.

Dual-culture assays on solid and liquid media revealed distinct interaction phenotypes, including distance inhibition and contact inhibition, reflecting competitive ecological strategies. LC–MS–based metabolomic profiling demonstrated that co-cultivation reshaped secondary metabolite production, leading to both suppression and induction of specific compounds. Signaling- and defense-related metabolites such as nicotinic acid, indole-3-acetic acid, and pyridoxine were differentially regulated during interaction. Notably, certain co-cultures triggered the production of metabolites absent in monocultures, including eleostearic acid and griseofulvin, indicating activation of previously silent or weakly expressed biosynthetic pathways.

Among the isolates, *P. nodositata* was identified as a natural producer of cryptotanshinone, a diterpenoid previously associated primarily with *Salvia* species. However, its production was modulated under interaction conditions, suggesting context-dependent metabolic regulation.

Collectively, these findings highlight the metabolic plasticity of root-associated endophytes and demonstrate that fungal–fungal interactions act as drivers of secondary metabolism reprogramming. The study underscores co-culture as an ecologically relevant strategy for uncovering interaction-mediated chemical diversity within plant-associated fungal communities.

1. Introduction

Plant-associated microorganisms are integral components of the plant holobiont, forming complex interaction networks that influence ecological fitness and secondary metabolism. Root tissues, in particular, represent dynamic ecological niches where microorganisms interact under spatial and nutritional constraints. *Salvia abrotanoides*, a medicinal plant with a well-developed root system, accumulates abietane-type diterpenoids, including tanshinones, which contribute to its pharmacological importance (Sairafianpour et al., 2001).

Tanshinones are bioactive diterpenoids widely reported from members of the genus *Salvia*, especially *Salvia miltiorrhiza* (Chang et al., 1986). These compounds exhibit diverse biological activities, including cardioprotective (Zhou et al., 1999), anti-inflammatory (Ma et al., 2016) and antidiabetic effects (Kim et al., 2007). Among them, cryptotanshinone, a quinoid diterpene with a nor-abietane skeleton, is particularly notable for its antitumor properties against various human cancer cell lines (Hu et al., 2015). Due to the valuable pharmacological potential of tanshinones, significant efforts have been made to enhance their production, including plant tissue culture approaches (Zaker et al., 2015) and

cryptotanshinone nanocrystals preparation (Zhao et al., 2023). Figure 1 illustrates the chemical structures of two major tanshinones found in *S. abrotanoides*. While these compounds are traditionally regarded as plant-derived metabolites, increasing evidence suggests that endophytic fungi can influence host metabolite production at genetic and physiological levels (Ganie et al., 2022), raising important questions regarding metabolic exchange and ecological coordination within plant–microbe systems.

Endophytic fungi colonize internal plant tissues without causing apparent disease symptoms and participate in dynamic interactions with both their hosts and neighboring microorganisms. Such interactions can modulate gene expression and reshape biosynthetic pathways, ultimately affecting secondary metabolite production (Ganie et al., 2022). However, most studies investigating fungal metabolite biosynthesis rely on monoculture systems, which do not reflect the competitive and cooperative dynamics characteristic of natural microbial communities.

Co-culture approaches have emerged as experimental models to simulate microbial interactions and to explore chemically mediated competition (Oh et al., 2007). Within this ecological framework, microorganisms synthesize antibiotics and other defense-related metabolites as survival strategies (Williams and Vickers, 1986; Zhou et al., 2024). Importantly, co-cultivation may suppress constitutive metabolites or activate silent biosynthetic gene clusters that remain unexpressed under standard laboratory conditions (Oh et al., 2005). These interaction-driven metabolic shifts are particularly relevant in rhizosphere-associated fungal communities, where dense microbial populations compete for space and resources.

In this study, we investigated root-associated fungal endophytes isolated from *S. abrotanoides* to evaluate how fungal–fungal interactions influence secondary metabolism. Particular attention was given to *Penicillago nodositata*, identified here as a cryptotanshinone-producing endophyte. Furthermore, co-culture experiments involving *Paraphoma radicina*, *Penicillium murcianum*, *Penicillium canescens*, and *Coniolariella hispanica* were conducted to assess interaction phenotypes and metabolite shifts under solid and liquid conditions. By integrating metabolomic profiling with interaction assays, this study aims to elucidate how interspecific fungal interactions drive metabolic reprogramming within plant-associated microbial communities.

2. Materials and Methods

2.1. Plant name, Sampling, Materials, and Media

Salvia abrotanoides, previously known as *Perovskia abrotanoides* (Drew et al., 2017), belongs to the Lamiaceae family (wfo-0001428614) (official name: Barazambel, local name: Golkabood). Fresh roots of *Salvia abrotanoides* Kar. were collected at the flowering stage from the Zoshk area (N 36°16′58″, E 59°07′06″) in northeastern Iran. A voucher specimen was deposited at the Herbarium of Ferdowsi University of Mashhad, Iran, under voucher code 36763 (FUMH). The roots were carefully removed from

the soil and transported to the laboratory within 24 hours of harvesting, then stored at 4°C for further processing. Cryptotanshinone standard was obtained from Sigma-Aldrich (USA).

Malt extract agar (MEA) medium (30 g malt extract, 3 g soya peptone, 15 g agar, 1000 mL deionized water) was used for the isolation and cultivation of fungal endophytes. Potato extract glucose broth (PGB) medium (Carl Roth GmbH, Germany) was employed for fermentation. Both media were sterilized via autoclaving before use.

2.2. Isolation and Cultivation of Fungal Endophytes

The roots of *S. abrotanoides* were washed thoroughly with running water, followed by deionized water to remove soil and contaminants. The roots were then cut into 15 mm segments and surface-sterilized using a modified version of the Sun et al. (2014) method. The sterilization process included sequential immersion in 70% ethanol (1 min), sterile water (1 min), 2.5% sodium hypochlorite (3 min), sterile water (1 min), and 70% ethanol (30 s), followed by three rinses in sterile water (1 min each) to remove residual sterilants.

Under sterile conditions, root segments were allowed to surface-dry before plating. The sterile root fragments were then cut into ~ 5 mm pieces (both transversely and longitudinally) using a sterile razor and placed on MEA medium supplemented with streptomycin (100 mg L^{-1}) to prevent bacterial contamination. Petri dishes were sealed with Parafilm (PM-996, 4 in 125 Ft) and incubated at 25 ± 2°C. Fungal colonies emerging from the plant segments were monitored daily and isolated after approximately 2–3 weeks. The isolated fungi were subcultured onto fresh MEA plates to obtain pure cultures.

2.3. Molecular Identification of Endophytic Isolates

Fungal isolates were grown on fresh MEA for 5–7 days at 30°C. Mycelia were scraped directly, and genomic DNA was extracted using the phenol-chloroform method. The DNA extraction process included disruption of mycelia using glass beads (250 mg, 0.25–0.5 mm, and two beads of 2.85–3.45 mm) in DNA extraction buffer (200 mM Tris-HCl, 250 mM NaCl, 0.5% SDS) and sodium acetate (pH 5.2). Mycelia were disrupted by ribolysis (2 × 30 s, Ribolyser). DNA quality and quantity were assessed using a UV-Vis spectrophotometer (NanoDrop 2000c, Thermo Fisher Scientific, USA).

For molecular identification, the internal transcribed spacer (ITS) regions (ITS1 and ITS2) and the intervening 5.8S rRNA region were amplified and sequenced (LGC Genomics, Berlin, Germany). PCR amplification was performed using the TPersonal Combi Biometra Thermocycler (Biometra GmbH, Germany) with universal ITS primers: ITS1f (5’ CTT GGT CAT TTA GAG GAA GTA A 3’) and ITS4r (5’ TCC TCG GCT TAT TGA TAT GC 3’). PCR products were purified using the Wizard SV Gel and PCR Clean-Up System (Promega, Madison, WI, USA) and quantified via NanoDrop 2000c. The resulting sequences were aligned using MEGA5 software and compared against the NCBI BLASTn database for taxonomic identification.

2.4. Preparation of Mycelial Extracts

Fungal isolates were inoculated into 250-mL Erlenmeyer flasks containing 100 mL of PGB medium and incubated for 24 days at 30°C on a rotary shaker (105 rpm). Mycelia were separated by vacuum filtration using filter paper (Rotilabo® round filter, type 112 A, 47 mm, Carl Roth GmbH, Germany), then dried at 40°C. The dried mycelia were homogenized using a mortar and pestle, suspended in 0.5 mL ethyl acetate, and mechanically disrupted with precooled glass beads (-70°C) (three beads, 2.85–3.45 mm, and 250 mg, 0.25–0.5 mm) using a Ribolyser (2 × 40 s at 6 m/s). The homogenate was centrifuged (10 min, 13,000 rpm, 4°C), and 250 µL of the supernatant was collected and stored at 4°C for further analysis.

2.5. Co-Culture on Solid Substrates

Four fungi (*P. radicina, P. murcianum, P. canescens*, and *C. hispanica*), previously reported as cryptotanshinone producers (Teimoori-Boghsani et al., 2020), along with *P. nodositata*, were selected for co-culture assays. Isodiametric disks of fungal mycelia from pure cultures were inoculated bipolarly onto MEA plates. Petri dishes were incubated at 30°C for 35 days, and each pure culture was used as a blank control.

2.6. Co-Culture in Liquid Substrates

Liquid co-culture experiments were conducted using isodiametric fungal mycelial disks inoculated into 100 mL PGB medium and incubated at 30°C (105 rpm, 24 days). Filtration, homogenization, and extraction followed the procedures described above. Co-cultures were performed in triplicate, with pure cultures serving as blank controls.

2.7. HPLC-MS Analysis

Ethyl acetate extracts were analyzed using an HPLC-hybrid quadrupole-orbitrap mass spectrometer (Q Exactive; Thermo Scientific, Germany). Separation was performed on an Atlantis DC18, 2.1 × 100 mm column (Waters Corporation, USA) with aqueous formic acid (0.1%, v/v) as solvent A and formic acid (0.1%, v/v) in acetonitrile as solvent B. The sample injection volume was 20 µL with a flow rate of 0.3 mL min^{-1}. The gradient program was set as follows: 40% B (2 min), 100% B (15 min), 40% B (5 min), and a total runtime of 40 min.

Mass spectrometry was conducted in both positive and negative ionization modes, with a nominal mass resolving power of 100.0-1500 m/z. The AGC target was set to 1×10^6, and the maximum accumulation time was 200 ms. Electrospray ionization (ESI) conditions included a spray voltage of 3.1 kV and a capillary temperature of 330°C. The resolution was set to 70,000 for accurate mass analysis.

2.8. Statistical analysis

Statistical calculations were performed using SPSS v.20.0.0 (SPSS Inc., Chicago, IL, United States). Mean and error values were calculated from three independent replicates (n = 3) and the results were reported as means ± standard error.

3. Results

3.1. Isolation, Identification and Authentication of Endophytic Fungus

The roots of *S. abrotanoides* were used to isolate fungal endophytes. Over a two-week period, thirty-eight fungal endophytes were successfully isolated from the roots. Following sub-culturing, they were categorized based on morphological differences. Each fungal isolate was carefully observed to distinguish its unique characteristics and utilized for secondary metabolite extraction. Figure 2 presents two fungi isolated from a root sample.

The endophytic fungus, designated RZM14, was isolated from the roots of *S. abrotanoides* and identified based on morphological characteristics and molecular analysis. The fungus exhibited both surface and submerged hyphae on MEA medium, with a colony morphology characterized by white coloration and a growth rate of approximately 4 mm per day. The fungus demonstrated high sporulation activity during transmission. Molecular analysis of the ITS region of rDNA, including ITS1, ITS2, and the intervening 5.8S rRNA gene, revealed 99% similarity to *Penicillago nodositata* (GenBank: accession number NR-103703.1) and 100% query coverage to *Eurotiales sp*. (accession number KC007253.1). Despite 99% similarity to other related taxa such as *Chaetothyriales sp.* (accession number HQ607865.1), the molecular analysis strongly indicated its classification as *Penicillago nodositata*. The ITS-5.8S rDNA sequence has been deposited in GenBank under accession number MK367769.1.

3.2. HPLC-MS Analysis

Extracts of *S. abrotanoides* roots and its symbiotic fungi were analyzed to identify secondary metabolites. Ethyl acetate extracts from *S. abrotanoides* roots were subjected to HPLC-MS analysis, revealing a diverse range of compounds, particularly diterpenoids. Table 1 lists the secondary metabolites identified in the ethyl acetate extract, including their molecular weights, formulas, and retention times. The results confirmed the presence of abietane diterpenoids such as abietic acid (podocarpa), ferruginol, sugiol, pisiferal, tanshinone IIA, and cryptotanshinone. Additionally, sesquiterpene alloaromadendrene, thioxanthene (a xanthene derivative), and estradiol 3-methyl ether were detected. Dicarboxylic acids such as suberic acid and azelaic acid were also identified (Table 1).

Table 1
Secondary metabolites produced by *S. abrotanoides* and *Penicillago nodositata*.

Name	Compound	Molecular weight (g/mol)	Formula	Retention time (min)
S. abrotanoides	Suberic acid	174.088	C8 H14 O4	1.509
	Azelaic acid	188.104	C9 H16 O4	1.678
	Alloaromadendrene	204.35	C15 H24	7.488
	Phenanthrene	178.23	C14 H10	13.462
	Abietic acid	302.5	C20 H30 O2	15.754
	Ferruginol	286.45	C20 H30 O	15.811
	Thioxanthene	198.28	C13 H10 S	16.17
	Estradiol 3-methyl ether	286.193	C19 H26 O2	17.925
	Sugiol	300.4	C20 H28 O2	18.172
	Tanshinone IIA	294.125	C19 H18 O3	18.906
	Pisiferal	300.208	C20 H28 O2	19.069
	Cryptotanshinone	296.141	C19 H20 O3	19.562
P. nodositata (RZM14)	Indole 3-acetic acid	175.063	C10 H9 N O2	1.365
	Picolinic acid	123.03	C6 H5 N O2	1.446
	Suberic acid	174.088	C8 H14 O4	1.509
	Solanidine	397.334	C27 H43 N O	1.789
	Cryptotanshinone	296.141	C19 H20 O3	10.976
	Hexamethylenetetramine	140.106	C6 H12 N4	36.756

Both *S. abrotanoides* root extracts and fungal biomass were examined for tanshinones. The samples were analyzed for 40 minutes using an LC-MS system. The molecular masses of the detected compounds were compared with authentic standards. Cryptotanshinone was identified based on the detection of a product ion of m/z 297.18059 for *S. abrotanoides* roots and m/z 297.14835 for RZM14, in comparison to m/z 297.14807 for the cryptotanshinone standard. Similarly, tanshinone IIA was identified with an m/z of 294.12564 for *S. abrotanoides* roots, compared to m/z 294.12578 for the tanshinone IIA standard. Quantitative analysis by LC-MS indicated cryptotanshinone yields of 0.170511 ± 0.004756 mg/g dry weight for fungal mycelia and 5.456071 ± 0.210159 mg/g dry weight for *S. abrotanoides* roots. The tanshinone IIA content in *S. abrotanoides* roots was 0.796395 ± 0.010412 mg/g dry weight (Table 2). The fragmentation pattern of cryptotanshinone is illustrated in Fig. 3.

Table 2
Mass and contents of cryptotanshinone and tanshinone IIA in *S. abrotanoides* and *Penicillago nodositata* (RZM14).

Name	Cryptotanshinone MS2 product ion (*m/z*)	Cryptotanshinone content (mg/g DW)	Tanshinone IIA MS2 product ion (*m/z*)	Tanshinone IIA content (mg/g DW)
S. abrotanoides	297.18059	5.456071 ± 0.210159	294.12564	0.796395 ± 0.010412
P. nodositata (RZM14)	297.14835	0.170511 ± 0.004756	-	-

Concentration of cryptotanshinone and tanshinone IIA measured in three replicates (n = 3). Values are presented as mean ± standard error of the mean (SEM).

Qualitative assays of mycelial extracts from RZM14 demonstrated chemical diversity in its metabolite profile. LC-MS analysis confirmed the presence of valuable compounds, including cryptotanshinone, solanidine, hexamethylenetetramine, indole-3-acetic acid, suberic acid, and picolinic acid (Table 1).

3.3. Co-Culture Studies

3.3.1. Co-Culture *of Penicillago nodositata* and *Penicillium murcianum*

Comparative analysis of pure and co-cultures of *P. nodositata* and *P. murcianum* revealed distinct growth patterns (Fig. 4C). In liquid co-culture, *P. murcianum* exhibited greater morphological dominance, as evidenced by the medium's color change (Fig. 4F). Secondary metabolite analysis indicated that hexadecanamide, suberic acid, and pantothenic acid were synthesized in both single and co-cultures. Azelaic acid was exclusively produced in *P. nodositata* pure culture. Overall, *P. murcianum* exhibited greater metabolite diversity than *P. nodositata*, synthesizing nicotinic acid, pyridoxine, nipecotic acid, and arabitol in both pure and co-cultures. Monoolein and xylitol were unique to *P. murcianum*. Griseofulvin was detected only in the co-culture (Table 3).

Table 3
Secondary metabolites produced in the pure and co-cultures of *Penicillago nodositata* and *Penicillium murcianum*. Squares indicate the excretion of specific compounds in pure and co-cultures.

Compounds	**Fungi**		
	Penicillago nodositata	***Penicillium murcianum***	***Penicillago nodositata + Penicillium murcianum***
Hexadecanamide	*	*	*
Azelaic acid	*		
Monoolein		*	
Nicotinic acid		*	*
Pyridoxine		*	*
Suberic caid	*	*	*
Nipecotic acid		*	*
Pantothenic acid	*	*	*
Xylitol		*	
Arabitol		*	*
Griseofulvin			*

Stars indicate the excretion of specific compounds by distinct isolates and co-cultures.

3.3.2. Co-Culture of *Paraphoma radicina* and *Penicillium murcianum*

The pure and co-culture study of *P. radicina* and *P. murcianum* demonstrated restricted growth on solid substrate, with complete inhibition after 20 days (Supplementary Fig. 2). In liquid co-culture, mycelial growth was more closely associated with *P. murcianum* colonies (Fig. 5F). Secondary metabolite profiling showed that hexadecanamide, nicotinic acid, and pyridoxine were common across all cultures. Monoolein was absent in co-culture but present in both pure cultures. *P. radicina* synthesized indole-3-acetic acid and mevalonolactone, while *P. murcianum* produced suberic acid, pantothenic acid, arabitol, nipecotic acid, and xylitol. Notably, eleostearic acid, a saturated fatty acid, was exclusively found in co-culture (Table 4).

Table 4
Secondary metabolites produced in the pure and co-cultures of *Paraphoma radicina* and *Penicillium murcianum*. Squares indicate the excretion of specific compounds in pure and co-cultures.

Compounds	**Fungi**		
	Paraphoma radicina	***Penicillium murcianum***	***Paraphoma radicina + Penicillium murcianum***
Hexadecanamide	*	*	*
Indole-3-acetic acid	*		
Mevalonolactone	*		
Monoolein	*	*	
Nicotinic acid	*	*	*
Pyridoxine	*	*	*
Suberic caid		*	*
Nipecotic acid		*	
Pantothenic acid		*	*
Xylitol		*	
Arabitol		*	*
Eleostearic acid			*

Stars indicate the excretion of specific compounds by distinct isolates and co-cultures.

3.3.3. Co-Culture of *Paraphoma radicina* and *Penicillago nodositata*

Analysis of *P. radicina* and *P. nodositata* cultures indicated that *P. nodositata* exhibited greater aggressiveness in solid substrate (Supplementary Fig. 3). In liquid co-culture, *P. nodositata* demonstrated superior morphological adaptation (Fig. 6F). Secondary metabolite analysis revealed that hexadecanamide was the only common metabolite. Pyridoxine was detected in *P. radicina* pure culture and co-culture. Additionally, *P. radicina* exclusively produced monoolein, nicotinic acid, indole-3-acetic acid, and mevalonolactone, while *P. nodositata* and co-culture shared azelaic acid, suberic acid, and pantothenic acid (Table 5).

Table 5
Secondary metabolites produced in the pure and co-cultures of *Paraphoma radicina* and *Penicillago nodositata*. Squares indicate the excretion of specific compounds in pure and co-cultures.

Compounds	**Fungi**		
	Paraphoma radicina	***Penicillago nodositata***	***Paraphoma radicina + Penicillago nodositata***
Hexadecanamide	*	*	*
Azelaic acid		*	*
Monoolein	*		
Nicotinic acid	*		
Pyridoxine	*		*
Suberic caid		*	*
Endole-3-acetic acid	*		
Pantothenic acid		*	*
Mevalonolactone	*		

Stars indicate the excretion of specific compounds by distinct isolates and co-cultures.

3.3.4. Co-Culture of *Penicillium canescens* and *Coniolariella hispanica*

In solid substrate, *C. hispanica* exhibited higher growth rates than *P. canescens*. Upon interaction, *P. canescens* mycelium changed from green to white and black (Supplementary Fig. 4). In liquid co-culture, the medium displayed characteristics of both pure cultures, but mycelial growth was significantly reduced, resulting in a muddy appearance (Fig. 7F). Secondary metabolite analysis confirmed the presence of hexadecanamide, pyridoxine, and suberic acid in all cultures. Nipecotic acid and arabitol were synthesized in both *P. canescens* and *C. hispanica* but were absent in co-culture. Indole-3-acetic acid was found in *P. canescens* and co-culture. Griseofulvin and mannitol were exclusive to *P. canescens*, while nicotinic acid, pantothenic acid, xylitol, and mevalonolactone were specific to *C. hispanica* (Table 6).

Table 6
Secondary metabolites produced in the pure and co-cultures of *Penicillium canescens* and *Coniolariella hispanica*. Squares indicate the excretion of specific compounds in pure and co-cultures.

Compounds	**Fungi**		
	Penicillium canescens	***Coniolariella hispanica***	***Penicillium canescens + Coniolariella hispanica***
Hexadecanamid	*	*	*
Indole-3-acetic acid	*		*
Nicotinic acid		*	
Pyridoxine	*	*	*
Suberic caid	*	*	*
Nipecotic acid	*	*	
Pantothenic acid		*	
Xylitol		*	
Arabitol	*	*	
Griseofulvin	*		
Mannitol	*		*
Mevalonolactone		*	

Stars indicate the excretion of specific compounds by distinct isolates and co-cultures.

4. Discussion

This study reports, for the first time, the isolation of *Penicillago nodositata* from *Salvia abrotanoides* and demonstrates its ability to produce bioactive compounds under cell-free fermentation conditions. We hypothesized that the metabolic capacity of this endophyte reflects a functionally integrated symbiotic relationship with its host plant, potentially contributing to the host's chemical defense and ecological adaptation. Our findings support the concept that endophytic fungi act not merely as passive inhabitants but as active metabolic partners and reservoirs of ethnopharmacologically relevant compounds. Numerous therapeutic metabolites have been documented from endophytic microorganisms, including paclitaxel (Stierle et al., 1993), camptothecin (Puri et al., 2005), maytansine (Wings et al., 2013), quercetin (Das et al., 2018), and cryptotanshinone (Teimoori-Boghsani et al., 2020), reinforcing the ecological and evolutionary significance of plant–fungus associations.

The discovery that fungi can biosynthesize diterpenoids such as cryptotanshinone carries important implications for understanding metabolic convergence within symbiotic systems. Cryptotanshinone,

known for its pro-apoptotic and anticancer properties (Wu et al., 2016), suggests that endophytes may participate in or complement host secondary metabolism. From a symbiotic perspective, fungal production of plant-associated metabolites may enhance host defense while simultaneously providing ecological advantages to the fungus. Furthermore, fungal-based production systems reduce dependency on plant harvesting and shorten cultivation periods of *S. abrotanoides*, offering a sustainable alternative for bioactive compound production (Kusari and Spiteller, 2012). Considering that endophytic community composition varies across geographical regions, the metabolic plasticity of such associations may represent adaptive responses to local environmental pressures.

In higher plants, isoprenoid biosynthesis proceeds via the cytosolic mevalonate (MVA) pathway and the plastidial methylerythritol phosphate (MEP) pathway (Yan et al., 2009), both producing isopentenyl pyrophosphate as a universal precursor (Laule et al., 2003). Although tanshinones were initially believed to be synthesized predominantly through the MEP pathway, evidence indicates significant involvement of the MVA pathway and metabolic crosstalk (Ge and Wu, 2005). However, the biosynthetic origin of tanshinones in fungi remains largely unknown. We therefore propose that the ability of *P. nodositata* to produce diterpenoids may represent either convergent evolution of biosynthetic machinery or adaptive metabolic exchange shaped by long-term plant–fungus interaction.

The production of plant-like secondary metabolites by endophytes raises fundamental questions regarding evolutionary and mechanistic origins. Horizontal gene transfer has frequently been proposed as an explanation (Stierle et al., 1995). However, evidence from gibberellin biosynthesis suggests independent evolutionary pathways. Gibberellins, originally identified in the fungal pathogen *Fusarium fujikuroi*, were later shown to be synthesized through fungal-specific chemical and genetic routes distinct from those of higher plants (Yamaguchi, 2008). This example supports the hypothesis that similar metabolites in plants and fungi may arise from parallel evolution rather than direct gene transfer. Elucidating whether tanshinone biosynthesis in *P. nodositata* follows plant-like or fungal-specific routes remains a key question for future symbiosis research.

Given the medicinal relevance of secondary metabolites and the limited knowledge of the root metabolome of *S. abrotanoides*, this study also aimed to characterize the host's root chemistry within the context of its endophytic association. Phytochemical analysis confirmed the presence of abietane diterpenoids, including abietic acid (podocarpa), ferruginol, sugiol, pisiferol, tanshinone IIA, and cryptotanshinone. These results align with Sairafianpour et al. (2001), who reported quinoid diterpenes such as cryptotanshinone and related derivatives. Notably, alloaromadendrene was identified for the first time in the roots of *S. abrotanoides*. The richness of terpenoids in the host plant supports the hypothesis that its endophytic community may be metabolically adapted to a terpenoid-rich environment. Previous studies have focused mainly on aerial parts and essential oils (Kakhky et al., 2009; Ashraf et al., 2014), making this the first comprehensive report of root-associated metabolites in the context of fungal symbiosis.

Metabolite profiling of *P. nodositata* under cell-free fermentation revealed compounds derived primarily from the mevalonate and shikimate pathways, including solanidine, indole-3-acetic acid (IAA), and picolinic acid. Solanidine is a key precursor for pharmacologically active steroids (Nikolic and Stankovic, 2003), whereas IAA plays a central role in plant growth regulation, and its microbial production has been linked to plant growth promotion (Hoffman et al., 2013). Picolinic acid exhibits antimicrobial activities (Intaraudom et al., 2013). The coexistence of defense-related and growth-regulating metabolites suggests that *P. nodositata* may influence host physiology at multiple functional levels. We therefore propose that this endophyte may contribute to host fitness by modulating growth and enhancing stress tolerance, consistent with mutualistic symbiosis models.

Co-culture experiments were conducted to evaluate whether inter-fungal interactions modulate secondary metabolism, reflecting ecological competition within host tissues. Four classical interaction patterns were observed on solid media: distance inhibition, zone lines, contact inhibition, and overgrowth (Bertrand et al., 2014). The interactions between *P. nodositata* and *P. murcianum*, as well as between *P. radicina* and *P. murcianum*, were characterized by distance inhibition, suggesting chemically mediated competition. Metabolites such as pyridoxine, indole derivatives, and nicotinic acid—known for antifungal activity (Balasubramaniyan et al., 2013; Chitra et al., 2017; Saha et al., 2016)—likely contribute to these inhibitory effects.

Our study suggests that *P. nodositata* is an aggressive and fast-growing fungus, as evident from its pure culture characteristics. However, when co-cultured with *P. murcianum*, its growth was restricted, likely due to the antifungal compounds produced by *P. murcianum*, including arabitol, xylitol, pyridoxine, and nicotinic acid. Additionally, research has demonstrated that azelaic acid, produced by *P. nodositata*, also has antifungal properties (Le Lay et al., 2016). The interaction between *P. radicina* and *P. nodositata* on solid substrates indicated that *P. nodositata* was the dominant species, making partial contact with *P. radicina* after 29 days and subsequently inhibiting its growth. This interaction aligns with the contact inhibition type. Despite *P. radicina* possessing a richer metabolite profile compared to *P. nodositata*, the latter exhibited a higher invasive capacity. Research suggests that microbial invasiveness depends on various factors, including genetics, environmental conditions, hybridization, evolution, and epigenetic modifications (Zenni et al., 2017). Furthermore, the interaction between *P. canescens* and *C. hispanica* on solid media revealed that *C. hispanica* was the more aggressive species, following a contact inhibition pattern. Notably, *P. canescens* underwent a color change from green to white and black upon contact with *C. hispanica*. Although there is limited information on color changes in co-cultures, this phenomenon likely resulted from oxidation or other chemical reactions triggered as a defense mechanism.

Analysis of the secondary metabolite profiles of *P. nodositata* and *P. murcianum* in liquid culture showed that *P. murcianum* was more successful, likely due to its richer metabolite production. One of the key objectives of co-culture studies in biotechnology is the identification of novel compounds that are not produced in pure cultures. Notably, griseofulvin production in the *P. nodositata* and *P. murcianum* co-

culture is of particular interest, as this polyketide is widely used in the treatment of fungal skin infections in both humans and animals (Gull and Trinci, 1973).

The secondary metabolite profile of the *P. radicina* and *P. murcianum* co-culture closely resembled that of *P. murcianum*, indicating that *P. murcianum* was the dominant species in liquid media. This dominance is likely associated with its production of arabitol, which has been reported to enhance fungal invasiveness and pathogenicity (Krell et al., 2018). Additionally, *P. murcianum* produces abundant spores with long environmental persistence, and arabitol has been identified as a key component of fungal spores (Bauer et al., 2008). Interestingly, eleostearic acid, an isomer of linoleic acid, was detected exclusively in the *P. radicina* and *P. murcianum* co-culture, suggesting it as a novel compound. Studies have shown that eleostearic acid possesses tumor-inhibitory properties (Tsuzuki et al., 2004). These findings align with previous reports documenting the production of novel metabolites in fungal co-cultures (Zhou et al., 2018; Li et al., 2019; Xu et al., 2023).

Interestingly, cryptotanshinone was not detected in co-culture conditions. This absence may reflect subculturing effects and metabolic silencing, phenomena commonly observed when endophytes are removed from their host environment. Kusari and Spiteller (2012) proposed that the loss of host-derived ecological cues can repress biosynthetic gene clusters through epigenetic mechanisms. This observation reinforces the hypothesis that full expression of fungal biosynthetic potential may depend on host-associated signals, underscoring the context-dependent nature of plant–fungus symbiosis.

5. Conclusion

This study provides the first evidence that *Penicillago nodositata*, isolated from *Salvia abrotanoides*, can produce bioactive metabolites including cryptotanshinone under cell-free fermentation conditions. Our findings support the hypothesis that endophytic fungi function as metabolically integrated partners within medicinal plants, contributing to host chemical ecology and adaptive fitness. Co-culture experiments further demonstrate that fungal interactions modulate secondary metabolism, potentially activating silent biosynthetic pathways and generating novel compounds. Collectively, these results highlight the ecological, evolutionary, and biotechnological significance of plant–fungus symbiosis and underscore the importance of studying endophytic metabolism within an interaction-driven framework.

Abbreviations

ITS
Internal transcribed spacer region
LC/MS
liquid chromatography-mass spectrometry
PGB
Potato glucose broth
HPLC-MS

High-performance liquid chromatography-mass spectrometry
MVA
Mevalonate pathway
MEP
Methylerythritol phosphate pathway

Declarations

Competing interest: The authors declare that they have no conflict of interests.

Funding: This work received funding from Ferdowsi University of Mashhad, Mashhad- Iran, through grant number 3/44714.

Acknowledgments

We would like to express our sincere gratitude to Arezoo Tazik (Department of Pharmacognosy, Mashhad University of Medical Sciences, Iran) for her help with fungal identification.

CRediT authorship contribution statement

Yeganeh Teimoori-Boghsani: Data curation, Formal analysis, Investigation, Methodology, Writing – original draft. **Ali Ganjeali:** Formal analysis, Resources, Software, Supervision, Writing – review and editing. **Gabriele Berg:** Funding acquisition, Resources, Supervision. **Tomislav Cernava:** Formal analysis, Methodology, Project administration. **Javad Asili:** Conceptualization, Formal analysis, Supervision. **Fatemeh Masoudi-Khorasani:** Data curation, Investigation. **Nasrin Moshtaghi:** Formal analysis, Methodology.

References

1. Ashraf SN, Zubair M, Rizwan K, Tareen RB, Rasool N, Zia-Ul-Haq M, Ercisli S (2014) Compositional studies and biological activities of *Perovskia abrotanoides* Kar. oils. Biol Res 47:12. https://doi.org/10.1186/0717-6287-47-12
2. Balasubramaniyan S, Paulraj A, Rajasekar K (2013) Synthesis, spectral characterization and antifungal activities of Cr (III), Co (II), Ni (II) and Hg (II) complexes with nicotinic acid hydrazide and azide as ligands. Res J Pharm Sci 2(3):1–6
3. Bauer H, Claeys M, Vermeylen R, Schueller E, Weinke G, Berger A, Puxbaum H (2008) Arabitol and mannitol as tracers for the quantification of airborne fungal spores. Atmos Environ 42(3):588–593. https://doi.org/10.1016/j.atmosenv.2007.10.013
4. Bertrand S, Bohni N, Schnee S, Schumpp O, Gindro K, Wolfender JL (2014) Metabolite induction via microorganism co-culture: a potential way to enhance chemical diversity for drug discovery. Biotechnol Adv 32(6):1180–1204. https://doi.org/10.1016/j.biotechadv.2014.03.001

5. Chang HM, But PP, Yao SC (1986) Pharmacology and applications of Chinese materia medica (Vol. 1): *World Scientific*
6. Chitra G, Franklin DS, Sudarsan S, Sakthivel M, Guhanathan S (2017) Indole-3-acetic acid/diol based pH-sensitive biological macromolecule for antibacterial, antifungal and antioxidant applications. Int J Biol Macromol 95:363–375. https://doi.org/10.1016/j.ijbiomac.2016.11.068
7. Das M, Prakash HS, Nalini MS (2018) Bioactive sesquiterpene, plasticizer, and phenols from the fungal endophytes of *Polygonum chinense* L. Ann Microbiol 68:595–609. https://doi.org/10.1007/s13213-018-1367-6
8. Drew BT, González-Gallegos JG, Xiang CL, Kriebel R, Drummond CP, Walker JB, Sytsma KJ (2017) Salvia united: The greatest good for the greatest number. Taxon 66(1):133–145. https://doi.org/10.12705/661.7
9. Ganie SA, Bhat JA, Devoto A (2022) The influence of endophytes on rice fitness under environmental stresses. Plant Mol Biol 109(4):447–467. https://doi.org/10.1007/s11103-021-01219-8
10. Ge X, Wu J (2005) Tanshinone production and isoprenoid pathways in *Salvia miltiorrhiza* hairy roots induced by Ag^{+} and yeast elicitor. Plant Sci 168:487–491. https://doi.org/10.1016/j.plantsci.2004.09.012
11. Gull K, Trinci APJ (1973) Griseofulvin inhibits fungal mitosis. Nature 244(5414):292–294. https://doi.org/10.1038/244292a0
12. Hoffman MT, Gunatilaka MK, Wijeratne K, Gunatilaka L, Arnold AE (2013) Endohyphal bacterium enhances production of indole-3-acetic acid by a foliar fungal endophyte. PLoS ONE 8(9):e73132. https://doi.org/10.1371/journal.pone.0073132
13. Hu T, Wang L, Zhang L, Lu L, Shen J, Chan RL, Li M, Wu WK, To KW, Cho CH (2015) Sensitivity of apoptosis-resistant colon cancer cells to tanshinones is mediated by autophagic cell death and p53-independent cytotoxicity. Phytomedicine 22(5):536–544. https://doi.org/10.1016/j.phymed.2015.03.010
14. Intaraudom C, Boonyuen N, Suvannakad R, Rachtawee P, Pittayakhajonwut P (2013) Penicolinates A–E from endophytic *Penicillium* sp. BCC16054. Tetrahedron Lett 54(8):744–748. https://doi.org/10.1016/j.tetlet.2012.11.028
15. Kakhky AM, Rustaiyan A, Masoudi S, Tabatabaei-Anaraki M, Salehi HR (2009) Composition of the essential oil of *Perovskia abrotanoides* Karel. and *Mentha longifolia* L. from Iran. J Essent Oil Bear Plants 12:205–212. https://doi.org/10.1080/0972060X.2009.10643712
16. Kim EJ, Jung SN, Son KH, Kim SR, Ha TY, Park MG, Jo IG, Park JG, Choe W, Kim S, HA J (2007) Anti-diabetes and anti-obesity effect of cryptotanshinone via activation of AMP-activated protein kinase. Mol Pharmacol 72(1):62–72. https://doi.org/10.1124/mol.107.034447
17. Krell V, Jakobs-Schoenwandt D, Persicke M, Patel AV (2018) Endogenous arabitol and mannitol improve shelf life of encapsulated *Metarhizium brunneum*. World J Microbiol Biotechnol 34(8):115. https://doi.org/10.1007/s11274-018-2492-x

18. Kusari S, Spiteller M (2012) Metabolomics of endophytic fungi producing associated plant secondary metabolites: Progress, challenges, and opportunities. In *Metabolomics*, 263–292. Springer, Dordrecht
19. Laule O, Fürholz A, Chang HS, Zhu T, Wang X, Heifetz PB, Gruissem W, Lange M (2003) Crosstalk between cytosolic and plastidial pathways of isoprenoid biosynthesis in *Arabidopsis thaliana*. *Proc. Natl. Acad. Sci. U.S.A.* 100, 6866–6871. https://doi.org/10.1073/pnas.1031755100
20. Le Lay C, Coton E, Le Blay G, Chobert JM, Haertlé T, Choiset Y, Van Long NN, Meslet-Cladière L, Mounier J (2016) Identification and quantification of antifungal compounds produced by lactic acid bacteria and propionibacteria. Int J Food Microbiol 239:79–85. https://doi.org/10.1016/j.ijfoodmicro.2016.06.020
21. Li HT, Zhou H, Duan RT, Li HY, Tang LH, Yang XQ, Yang YB, Ding ZT (2019) Inducing secondary metabolite production by co-culture of the endophytic fungus *Phoma* sp. and the symbiotic fungus *Armillaria* sp. J Nat Prod 82(4):1009–1013. https://doi.org/10.1021/acs.jnatprod.8b00685
22. Ma S, Zhang D, Lou H, Sun L, Ji J (2016) Evaluation of the anti-inflammatory activities of tanshinones isolated from *Salvia miltiorrhiza* var. alba roots in THP-1 macrophages. J Ethnopharmacol 188:193–199. https://doi.org/10.1016/j.jep.2016.05.018
23. Nikolic NC, Stankovic MZ (2003) Solanidine hydrolytic extraction and separation from the potato (*Solanum tuberosum* L.) vines by using solid–liquid–liquid systems. J Agric Food Chem 51:1845–1849. https://doi.org/10.1021/jf020426s
24. Oh DC, Jensen PR, Kauffman CA, Fenical W (2005) Libertellenones A–D: induction of cytotoxic diterpenoid biosynthesis by marine microbial competition. Bioorg Med Chem 175267–5273. https://doi.org/10.1016/j.bmc.2005.05.068
25. Oh DC, Kauffman CA, Jensen PR, Fenical W (2007) Induced production of emericellamides A and B from the marine-derived fungus Emericella sp. in competing co-culture. J Nat Prod 70(4):515–520. https://pubs.acs.org/doi/10.1021/np060381f
26. Puri SC, Verma V, Amna T, Qazi GN, Spiteller M (2005) An endophytic fungus from *Nothapodytes foetida* that produces camptothecin. J Nat Prod 68:1717–1719. https://doi.org/10.1021/np0502802
27. Saha H, Pal AK, Sahu NP, Saha RK (2016) Feeding pyridoxine prevents *Saprolegnia parasitica* infection in fish *Labeo rohita*. Fish Shellfish Immunol 59:382–388. https://doi.org/10.1016/j.fsi.2016.09.045
28. Sairafianpour M, Christensen J, Stærk D, Budnik BA, Kharazmi A, Bagherzadeh K, Jaroszewski JW (2001) Leishmanicidal, antiplasmodial, and cytotoxic activity of novel diterpenoid 1, 2-quinones from *Perovskia abrotanoides*: new source of tanshinones. J Nat Prod 64(11):1398–1403. https://pubs.acs.org/doi/10.1021/np010032f
29. Stierle A, Strobel G, Stierle D (1993) Taxol and taxane production by *Taxomyces andreanae*, an endophytic fungus of Pacific yew. Science 260:214. 10.1126/science.8097061
30. Stierle A, Strobel G, Stierle D, Grothaus P, Bignami G (1995) The search for a taxol-producing microorganism among the endophytic fungi of the Pacific yew, *Taxus brevifolia*. J Nat Prod

58:1315–1324. https://doi.org/10.1021/np50123a002

31. Sun J, Xia F, Cui L, Liang J, Wang Z, Wei Y (2014) Characteristics of foliar fungal endophyte assemblages and host effective components in *Salvia miltiorrhiza* Bunge. Appl Microbiol Biotechnol 98(7):3143–3155. https://doi.org/10.1007/s00253-013-5300-4
32. Teimoori-Boghsani Y, Ganjeali A, Cernava T, Müller H, Asili J, Berg G (2020) Endophytic fungi of native *Salvia abrotanoides* plants reveal high taxonomic diversity and unique profiles of secondary metabolites. Front Microbiol 10:3013. https://doi.org/10.3389/fmicb.2019.03013
33. Tsuzuki T, Tokuyama Y, Igarashi M, Miyazawa T (2004) Tumor growth suppression by α-eleostearic acid, a linolenic acid isomer with a conjugated triene system, via lipid peroxidation. Carcinogenesis 25(8):1417–1425. https://doi.org/10.1093/carcin/bgh109
34. Williams ST, Vickers JC (1986) The ecology of antibiotic production. Microb Ecol 12(1):43–52. https://doi.org/10.1007/BF02153221
35. Wings S, Müller H, Berg G, Lamshöft M, Leistner E (2013) A study of the bacterial community in the root system of the maytansine containing plant *Putterlickia verrucosa*. Phytochemistry 91:158–164. https://doi.org/10.1016/j.phytochem.2012.06.016
36. Wu CF, Klauck SM, Efferth T (2016) Anticancer activity of cryptotanshinone on acute lymphoblastic leukemia cells. Arch Toxicol 90:2275–2286. https://doi.org/10.1007/s00204-015-1616-4
37. Xu S, Li M, Hu Z, Shao Y, Ying J, Zhang H (2023) The potential use of fungal co-culture strategy for discovery of new secondary metabolites. Microorganisms 11(2):464. https://doi.org/10.3390/microorganisms11020464
38. Yamaguchi S (2008) Gibberellin metabolism and its regulation. Annu Rev Plant Biol 59:225–251. https://doi.org/10.1146/annurev.arplant.59.032607.092804
39. Yan X, Zhang L, Wang J, Liao P, Zhang Y, Zhang R, Kai G (2009) Molecular characterization and expression of 1-deoxy-D-xylulose 5-phosphate reductoisomerase (DXR) gene from *Salvia miltiorrhiza*. Acta Physiol Plant 31:1015–1022. https://doi.org/10.1007/s11738-009-0320-5
40. Zaker A, Sykora C, Gössnitzer F, Abrishamchi P, Asili J, Mousavi SH, Wawrosch C (2015) Effects of some elicitors on tanshinone production in adventitious root cultures of *Perovskia abrotanoides* Karel. Ind Crops Prod 67:97–102. https://doi.org/10.1016/j.indcrop.2015.01.015
41. Zenni RD, Dickie IA, Wingfield MJ, Hirsch H, Crous CJ, Meyerson LA, Burgess TI, Zimmermann TG, Klock MM, Siemann E, Erfmeier A (2017) Evolutionary dynamics of tree invasions: complementing the unified framework for biological invasions. AoB Plants 9(1):plw085
42. Zhao W, Ruan B, Sun X, Yu Z (2023) Preparation and optimization of surface stabilized cryptotanshinone nanocrystals with enhanced bioavailability. Front Pharmacol 14:1122071. https://doi.org/10.3389/fphar.2023.1122071
43. Zhou GY, Zhao BL, Hou JW, Ma GE, Xin WJ (1999) Protective effects of sodium tanshinone IIA sulphonate against adriamycin-induced lipid peroxidation in mice heart *in vivo* and *in vitro*. Pharmacol Res 40(6):487–491. https://doi.org/10.1006/phrs.1999.0545

44. Zhou QY, Yang XQ, Zhang ZX, Wang BY, Hu M, Yang YB, Zhou H, Ding ZT (2018) New azaphilones and tremulane sesquiterpene from endophytic *Nigrospora oryzae* cocultured with *Irpex lacteus*. Fitoterapia 130:26–30. https://doi.org/10.1016/j.fitote.2018.07.018Get rights and content
45. Zhou X, Wang J, Huan Y, Jin T, Wang L, Zhao Y (2024) Fungal-bacterial co-culture enhanced the biodegradation of cholorobenzen in biotrickling filters: Analysis of performance and microbial characterization. J Water Process Eng 67:106181. https://doi.org/10.1016/j.jwpe.2024.106181

Figures

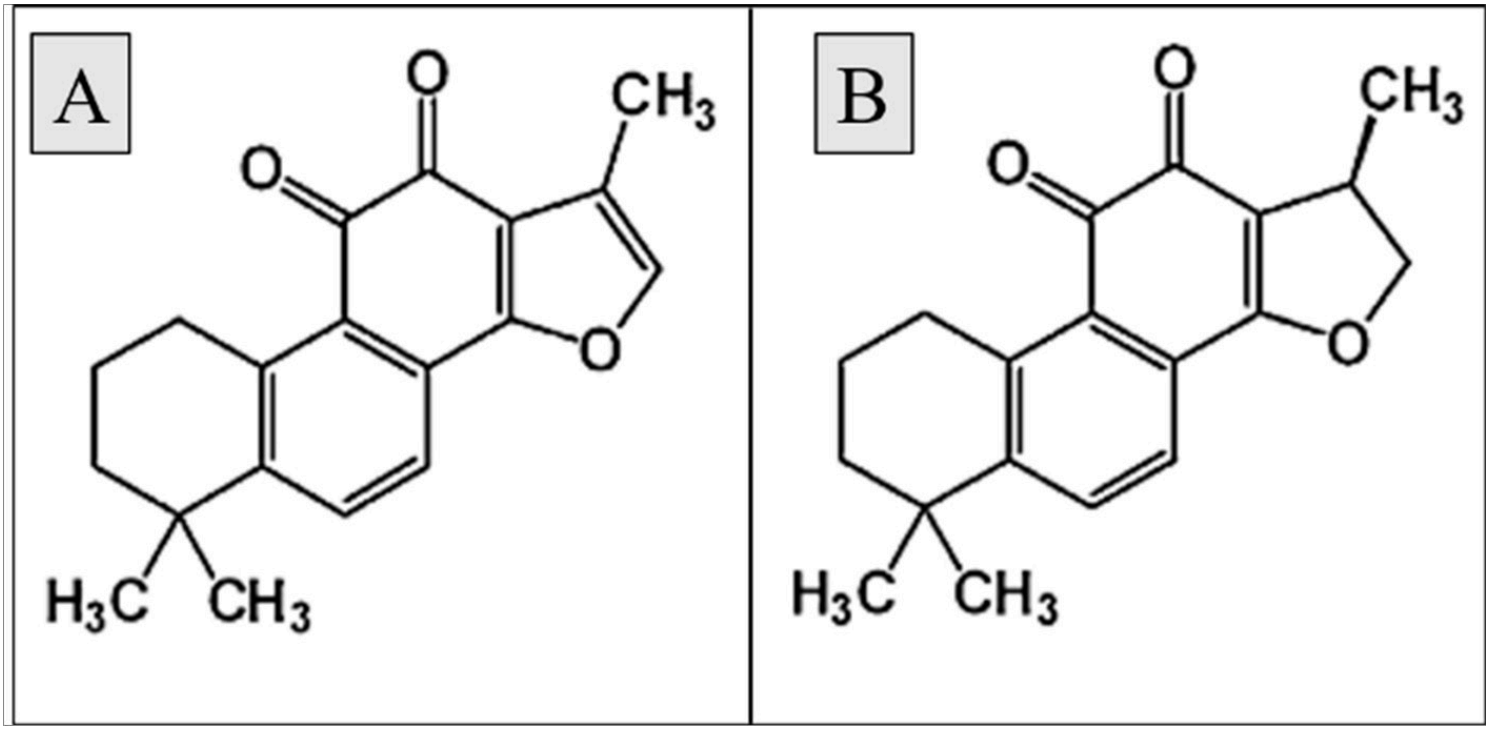


Figure 1

A and B show the structures of tanshinone IIA and cryptotanshinone respectively

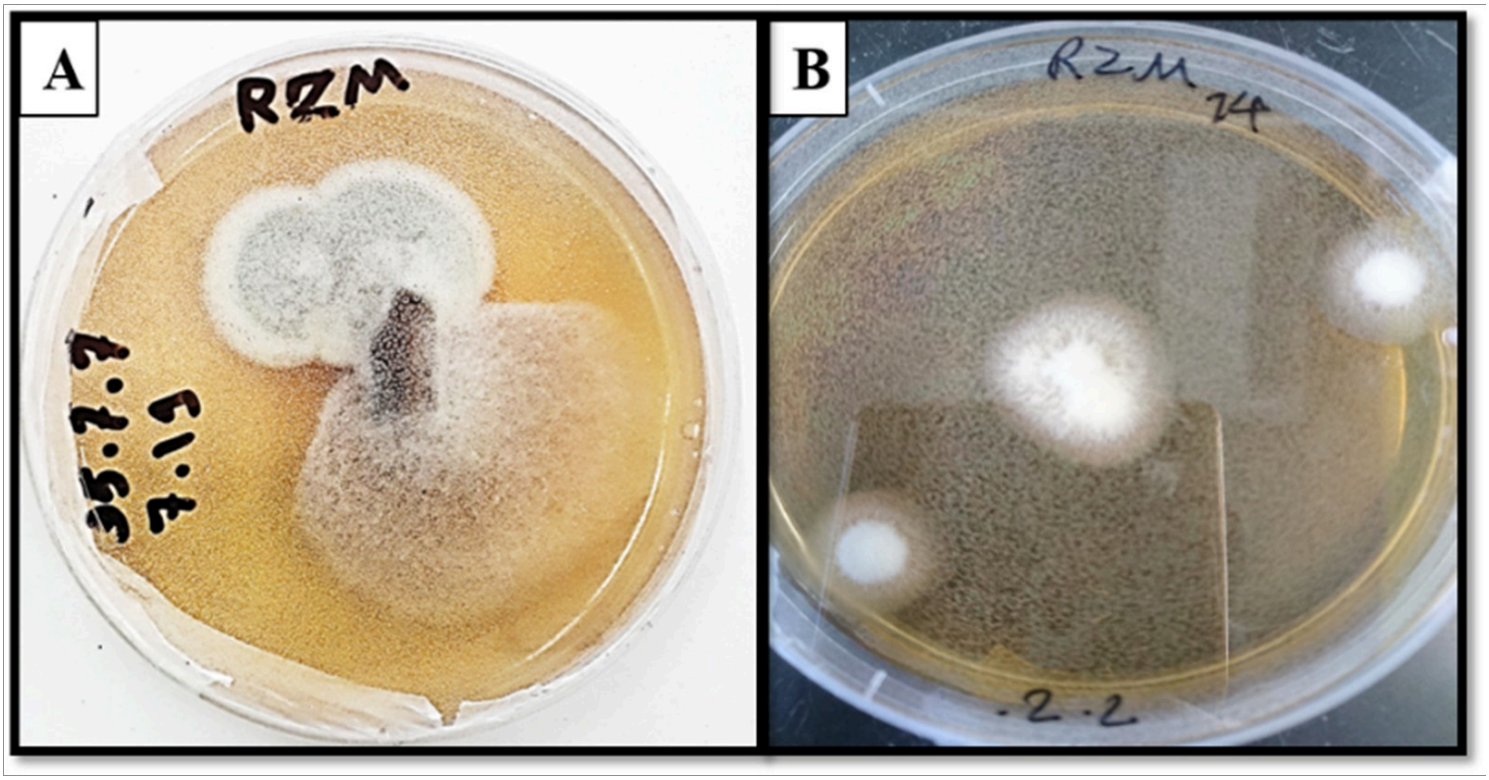


Figure 2

Endophytic fungi isolated from *S. abrotanoides*: A shows two fungi which have been released from a root sample after 2 weeks and B is the fungus which has been identified as the *Penicillago nodositata*

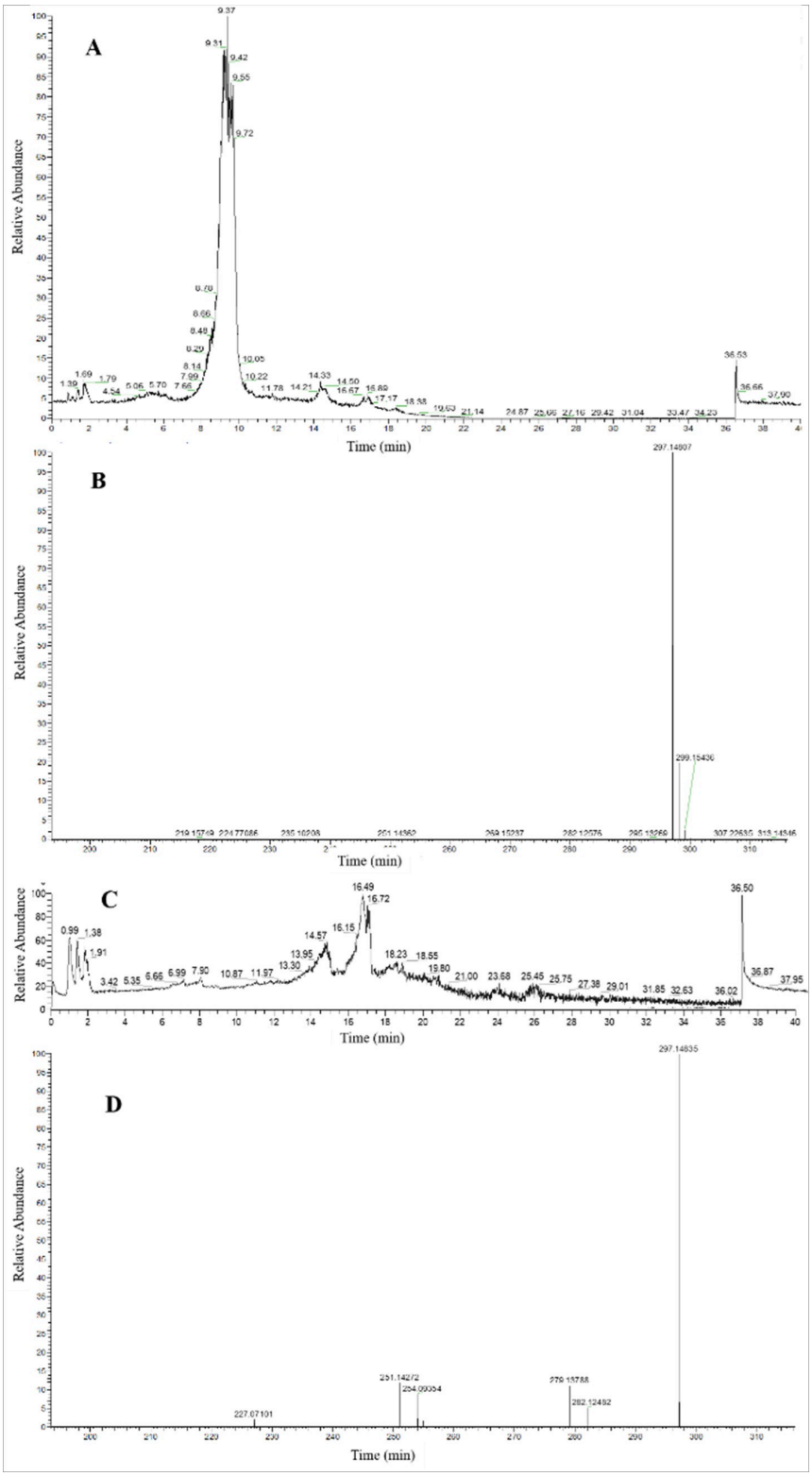


Figure 3

High-resolution MS2 product ions of cryptotanshinone: A and B are chromatogram and spectrum of Authentic reference standard, respectively; C and D are chromatogram and spectrum of cryptotanshinone produced by the endophytic fungus

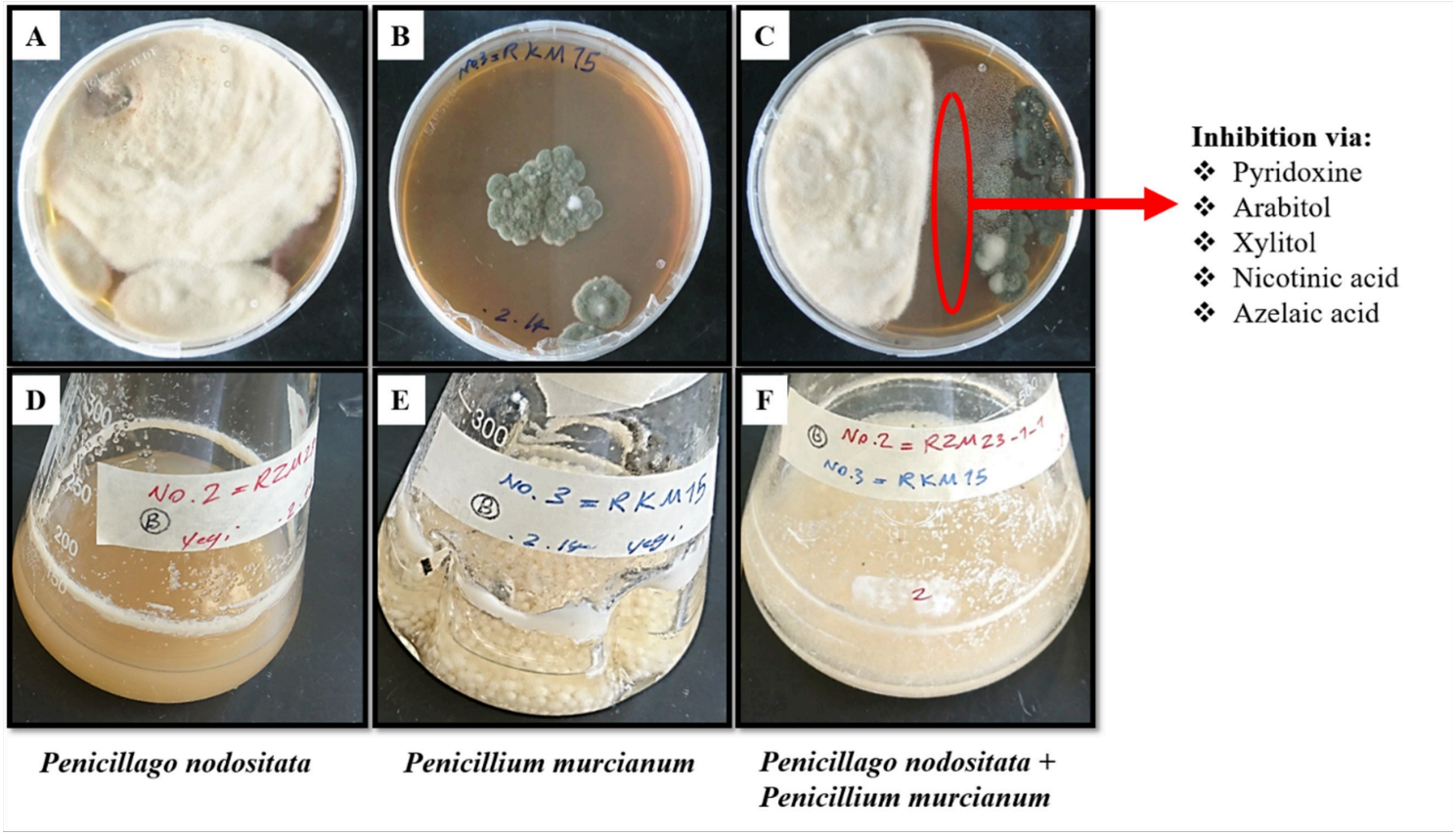


Figure 4

Solid and liquid cultures of *P. murcianum* and *P. nodositata*. A, B, D and E show the pure cultures of *P. nodositata*and *P. murcianum* in solid and liquid cultures respectively after 35 days. C and F show the co-culture of *P. nodositata* and *P. murcianum*in solid and liquid substrates respectively after 24 days. Red circle shows the distance inhibition

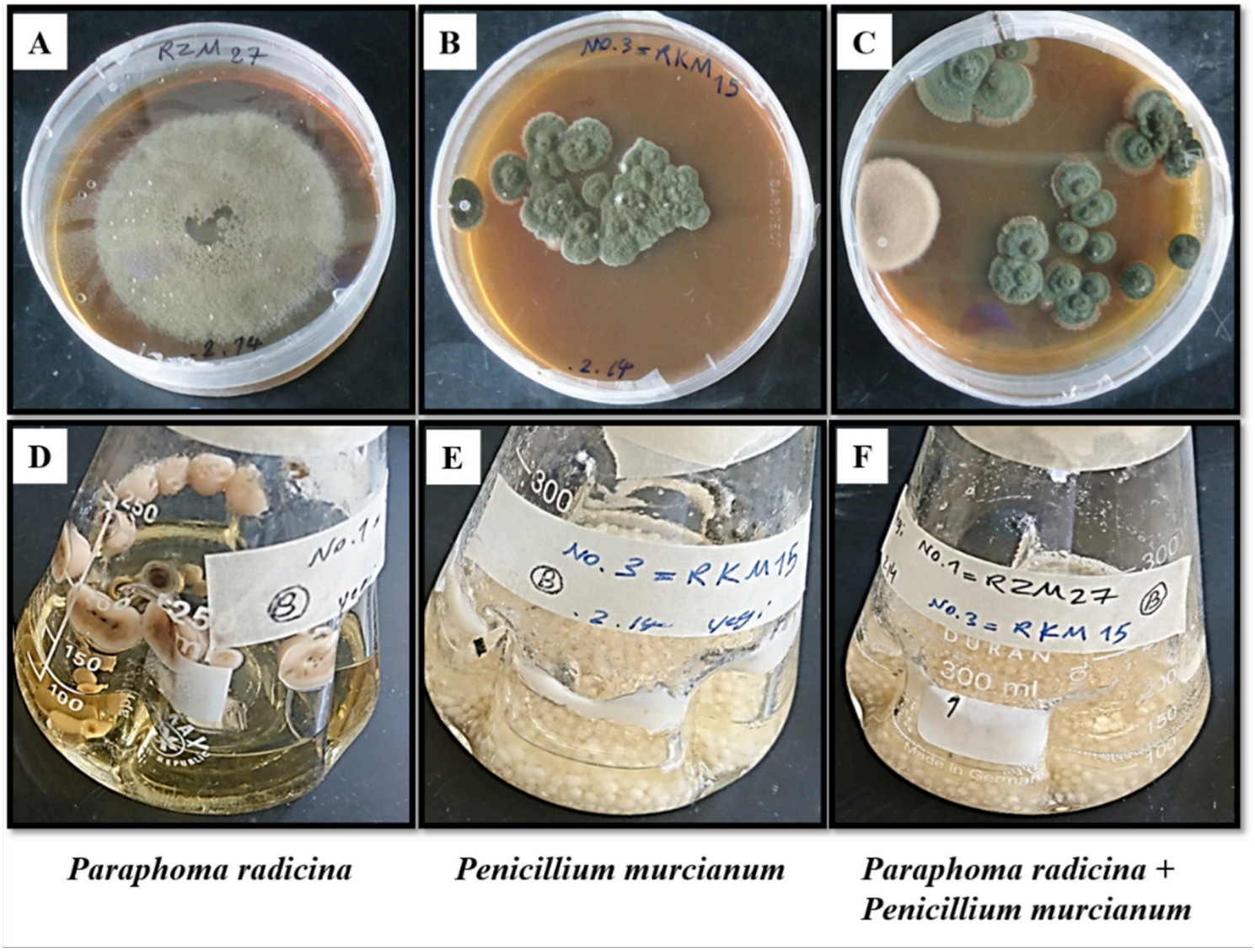


Figure 5

Solid and liquid cultures of *P. radicina* and *P. murcianum.* A, B, D and E show the pure cultures of *P. radicina* and *P. murcianum*in solid and liquid cultures respectively after 35 days. C and F show the co-culture of *P. radicina* and *P. murcianum* in solid and liquid substrates respectively after 24 days

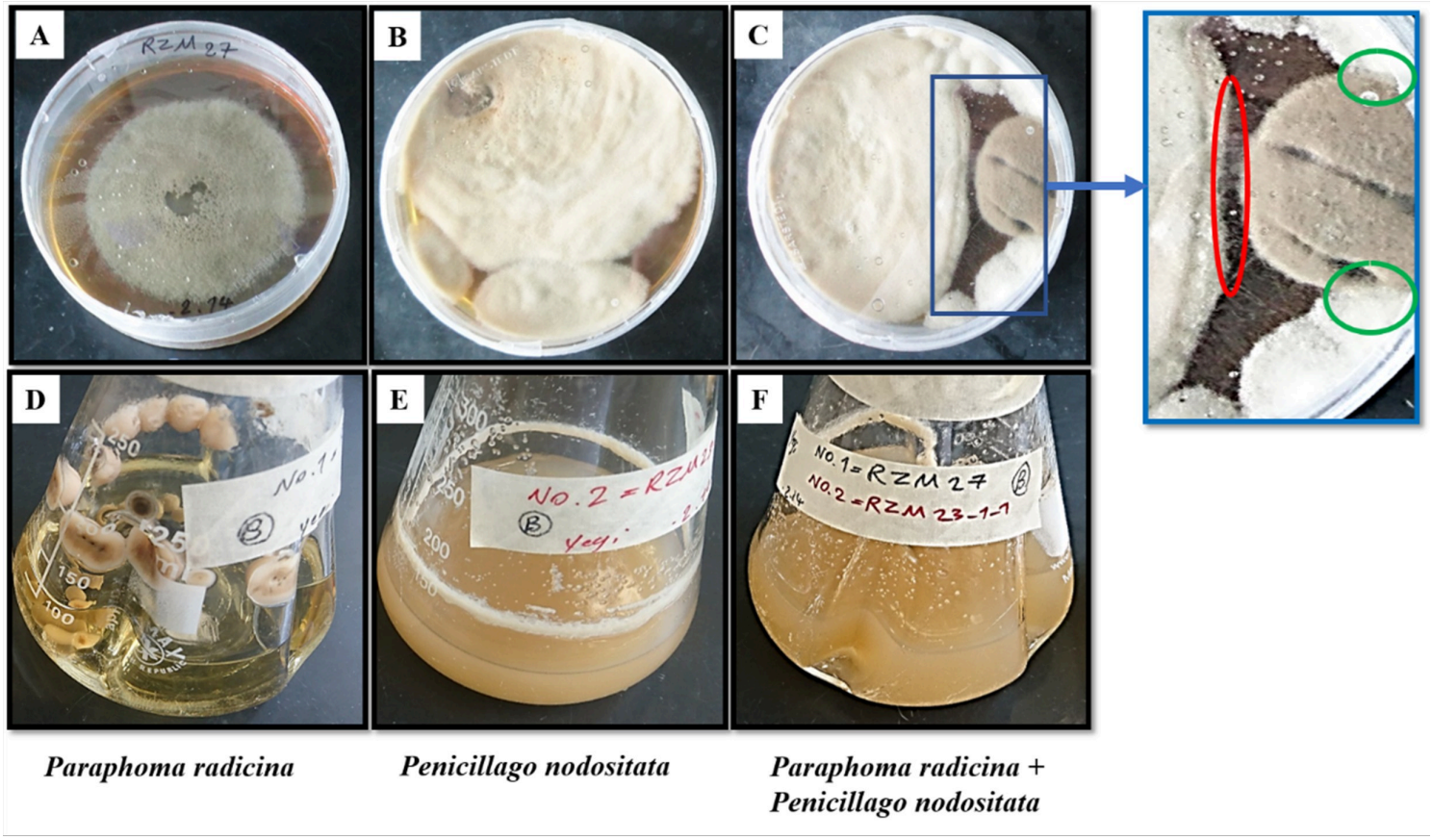


Figure 6

Solid and liquid cultures of *P. radicina* and *P. nodositata.*A, B, D and E show the pure cultures of *P. radicina* and *P. nodositata*in solid and liquid cultures respectively after 35 days. C and F show the co-culture of *P. radicina* and *P. nodositata* in solid and liquid substrates respectively after 24 days. Green circles show the contact inhibition

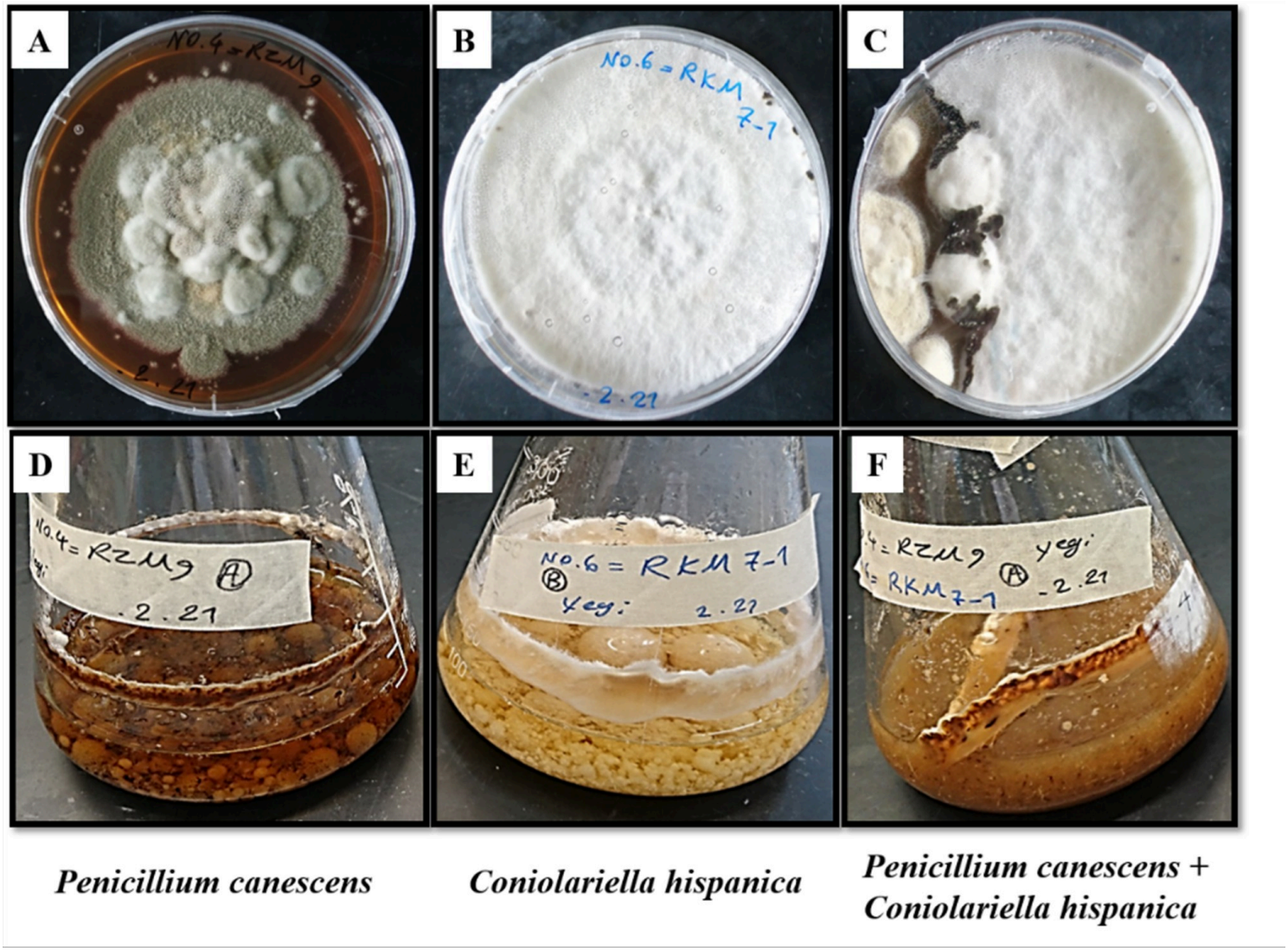


Figure 7

Solid and liquid cultures of *P. canescens*and *C. hispanica.* A, B, D and E show the pure cultures of *P. canescens* and *C. hispanica* in solid and liquid cultures respectively after 35 days. C and F show the co-culture of *P. canescens* and *C. hispanica* in solid and liquid substrates respectively after 24 days

Supplementary Files

This is a list of supplementary files associated with this preprint. Click to download.

- Supportinginformation.docx